Selective Deamidation of Recombinant Human Stem Cell Factor during in Vitro Aging: Isolation and Characterization of the Aspartyl and Isoaspartyl Homodimers and Heterodimers

Yueh-Rong Hsu, Wen-Chang Chang,‡ Elizabeth A. Mendiaz, Shinichi Hara, David T. Chow, Michael B. Mann, Keith E. Langley, and Hsieng S. Lu*

Amgen Inc., Amgen Center, 1840 DeHavilland Drive, Thousand Oaks, California 91320

Received September 24, 1997; Revised Manuscript Received December 9, 1997

ABSTRACT: During in vitro aging, deamidation of recombinant human stem cell factor produced in *Escherichia. coli* was detected by HPLC analysis and by the release of soluble ammonia. The deamidation rate is very slow in buffers at low pH or at low temperatures; however, the rate is significantly accelerated in alkaline buffers such as sodium bicarbonate in combination with elevated temperatures. HPLC isolation of various deamidated forms followed by peptide mapping and mass spectrometric analyses revealed that the deamidation involves Asn^{10} in the sequence -T^{9}NNV- near the N-terminus of the protein. Following peptide mapping analysis, significant amounts of aspartyl and isoaspartyl peptides were identified, indicating the conversion of asparagine into both aspartate and isoaspartate residues. As a result of spontaneous association−dissociation of stem cell factor dimer, a total of five deamidated forms, including two homodimers and three heterodimers, were detected and isolated. Cell proliferation assays showed that two rhSCF heterodimeric species, derived from dimerization between isoaspartyl and other stem cell factor monomers, retain only approximately half of the biological activity. The homodimer with isoaspartic acid in place of Asn^{10} is 50-fold less potent, while the aspartyl homodimer, either isolated during deamidation experiments or recombinantly prepared by site-directed mutagenesis (e.g., N10D and N10D/N11D variants), exhibits higher activity than the standard molecule. In comparison, synthetic N10A and N10E variants, though missing the deamidation site, are significantly less active. All these variants lacking the Asn^{10} deamidation site are relatively more stable than those containing the asparagine residue. The results indicate that the biological function and chemical stability of stem cell factor are influenced by the nature of the residue at position 10.

Stem cell factor (SCF),[1] also termed *KIT* ligand, mast cell growth factor, and Steel factor, is a hematopoietic growth factor acting on early stage hematopoietic cell lineages (*1*−*6*; for review, see refs *7*, *8*). The molecule is initially expressed as a membrane-associated form of 248 amino acids, and a soluble form of 165 amino acids is generated by proteolytic release from the extracellular domain of the membrane-bound form (*9*). However, a membrane-bound form of 220 amino acids derived from alternative splicing was also identified (*10*). Soluble SCF is glycosylated at one to three of the asparagine residues and also at three of the threonine/serine residues (*11*−*13*). Soluble recombinant human SCF (rhSCF) expressed in *Escherichia coli* is not glycosylated, but it exhibits normal SCF biological functions comparable to the glycosylated molecule (*12*). rhSCF forms a noncovalently associated dimer (*11*), with a determined dimer association constant of (2−4) × 10^{8} M^{-1} (*14*), and can spontaneously undergo monomer dissociation and reassociation in its native state (*15*). Epitope mapping analysis and immunoneutralization of rhSCF have recognized regions that are functionally important for SCF biological activity (*16*). Since rhSCF is able to synergize with other cytokines to stimulate growth of hematopoietic progenitors in vitro and to stimulate blood cell production in vivo (*7*, *8*, *17*), therapeutic evaluation of the molecule to aid mobilization of peripheral blood progenitor cells for autologous transplantation patients is under investigation (*18*).

Like many other proteins, rhSCF is prone to degradation reactions, such as deamidation of Asn residues. The spontaneous, nonenzymatic deamidation of Asn is perhaps the most frequently observed covalent modification in proteins during purification or storage (*19*−*21*). The susceptibility of Asn to deamidation has been shown to be affected by local three-dimensional structure and in particular by amino acids at the carboxyl side of the Asn deamidation site (*22*). From studies of synthetic peptides (*23*−*26*) and from extensive survey of known deamidation sites in proteins (*26*), Asn-Gly and Asn-Ser sequences appear to be most favorable for deamidation. A high deamidation rate also occurs at Asn residues with a Ser penultimate to the N-terminus (*26*). The mechanism of deamidation has been

* All correspondence should be addressed to this author at Amgen Inc., Mail Stop 14-2-E, Amgen Center, Thousand Oaks, CA 91320. Telephone: 805-447-3092. Fax: 805-499-7464. E.Mail: hlu@amgen.com.

‡ W.-C.C. is a visiting scientist at Amgen Inc. Current address: Institute of Biological Chemistry, Academia Sinica, P.O. Box 23-106, Taipei, Taiwan.

[1] Abbreviations: rhSCF, recombinant human stem cell factor; SP-, sulfopropyl; PTH, phenyl thiohydantoin; DTT, dithiothreitol; isoD, isoaspartate; IEF, isoelectric focusing.

S0006-2960(97)02372-6 CCC: $15.00
Published on Web 02/03/1998

proposed for Asn residues in proteins, based on the pioneering work on hydroxylamine cleavage of Asn−Gly bonds in proteins (*27*) and on the ability of the isoaspartate *O*-methyltransferase enzyme (EC 2.1.1.77) to catalyze methylation of Asn-deamidated peptides and proteins (*28*, *29*). The mechanism involves formation of a succinimide intermediate by nucleophilic attack on the amide carbonyl of Asn by the nitrogen of the peptide group linking the Asn to the following residue. As hydrolysis of the succinimide intermediate may occur on either side of the imide nitrogen, the Asp residue produced by the deamidation reaction will be linked to the subsequent residue by a normal α-aspartyl or by a β-aspartyl (or isoaspartyl) bond. In the latter case, the β-carbon is part of the polypeptide backbone, and the α-carboxyl group is present as an atypical one carbon carboxylic acid side chain available for methylation by isoaspartate *O*-methyltransferase. Under in vitro conditions, selective deamidation occurs in a number of purified proteins such as growth hormone (*30*), calmodulin (*31*), ribonuclease (*32*), and phosphocarrier protein (*33*). Robinson and Rudd proposed that deamidation can also occur in vivo, likely related to the aging of the protein (*34*). More recently, it has been reported that this is indeed the case for proteins such as triosephosphate isomerase (*35*), ribonuclease (*36*), lens crystallins (*37*), and hydroxymethyltransferase (*38*).

Formation of isoaspartyl residues, a reaction generated either during deamidation of Asn residues as described above or by direct isomerization of Asp residues, is a widespread form of peptide and protein degradation that can result in microheterogeneity and the loss of function and stability (*20*, *39*−*40*). For example, isomerization of Asp^{101} in lysozyme significantly reduces affinity for its chitin substrate (*41*). Isomerization of Asp^{11} in human epidermal growth factor reduces its mitogenic activity to 20% of normal (*42*), while isomerization of Asp^{32} in the light chain of a monoclonal antibody to human IgE significantly reduces its binding affinity to a high-affinity human IgE receptor (*43*). An isoaspartate form isolated from a phosphocarrier protein deamidated at Asn^{12} exhibits impaired phosphohydrolysis properties (*33*). Deamidation of bovine ribonuclease at Asn^{67} generates an isoaspartate isoform that has a lower catalytic activity and a slower refolding rate (*32*). X-ray crystallographic data of this isoform indicate considerable structural deviations in a disulfide loop region (residues 65−72). The insertion of an extra methylene group at residue 67 breaks up the hydrogen bond network that makes up a rather rigid structure in the region (*44*). An isoaspartate derivative of human growth hormone releasing factor formed by deamidation at Asn^{8} exhibits relatively low biological activity that is associated with a disrupted α-helical structure near the isopeptide bond (*45*). An isoaspartate derivative of calbindin generated by deamidation of Asn^{56} loses calcium binding by about 10-fold, and the aspartyl derivative actually binds calcium 50% more tightly than the native asparaginyl form (*46*).

Deamidation of Asn residues or isomerization of Asp residues has been shown to occur in a variety of protein-based pharmaceuticals including human growth hormone (*30*), tissue plasminogen activator (*47*), hirudin (*48*), monoclonal antibodies (*43*), acidic fibroblast growth factor (*49*), and interleukin 1 (*50*), with varying effect on the activity or stability of the drug. In this report, we demonstrate that the deamidation of rhSCF can be induced by prolonged storage at elevated temperature. Large quantities of acidic rhSCF isoforms accumulated when rhSCF was stored under alkaline buffer conditions. By isolation and structural analysis, we conclude that these acidic species arise from deamidation at Asn^{10}. The occurrence of multiple acidic forms detectable by ion-exchange HPLC is due to spontaneous dimer subunit exchange among native rhSCF and the two deamidated species. Reduction in biological activity was found in SCF species with an isoaspartyl residue in place of Asn^{10} or in N10A and N10E SCF variants made by site-directed mutagenesis. In contrast, increased activity (∼150% of normal) was found in rhSCF forms having Asp at position 10. The presence of Asn or Asp at position 10 appears to be critical for maintaining maximal rhSCF biological function.

MATERIALS AND METHODS

Materials. HPLC-grade water and acetonitrile were obtained from Burdick and Jackson. Protein sequencing reagents and solvents were supplied by Perkin-Elmer-Applied Biosystem Inc. (Foster City, CA).

E. coli Expression and Preparation of rhSCF. Procedures to construct the expression vector, the fermentation conditions for high-level expression of rhSCF, and the purification were reported previously (*10*). The gene for rhSCF has a methionine initiation codon followed by codons for human SCF^{1-165}. The purified rhSCF retains the initiating Met (position Met^{-1}). N10D, N10D/N11D, N10A, and N10E rhSCF variants were prepared similarly by site-directed mutagenesis as described (*51*).

Isoelectrofocusing (*IEF*) *Gel Electrophoresis*. rhSCF preparations were concentrated and buffer-exchanged into 2−5 mM sodium acetate buffer, pH 5.0, using Centricon 10 devices (Amicon). Samples were then spotted onto 0.4 mm (thickness) isoelectrofocusing gels containing LKB ampholine (pH 4−6), which were prepared on Gel Bond PAG films (Pharmacia) using an LKB 2217-200 Ultromould Gel Casting Unit as described (*52*). Electrophoresis, staining, and destaining were essentially identical with those described previously (*52*).

Deamidation Experiments. Deamidation experiments were carried out at different pHs under different buffer conditions. The following buffers were used: 100 mM sodium bicarbonate, pH 8.4; 40 mM Tris-HCl, pH 7.2; 10 mM sodium phosphate, pH 6.5; and 20 mM sodium acetate with or without 140 mM NaCl at pH 5.0. SCF samples were buffer-exchanged into the described buffers using a Centriprep device (Amicon) with a molecular mass cutoff of 10 kDa, at 5 °C. The buffer-exchanged SCF samples were incubated at 37 °C for 1−5 days, at which times samples were taken and analyzed by cation-exchange HPLC using an SP-5PW TSK gel (sulfopropyl [SP]) HPLC column as described below.

During deamidation experiments, the release of ammonia as a function of time was measured by an enzyme coupling assay using bovine glutamate dehydrogenase (Sigma Chemical Co.) as described (*53*). Recombinant hSCF concentration was 0.2 mM in these experiments.

Separation of Deamidated rhSCF Species. Separation of deamidated rhSCF isoforms was performed by cation-exchange HPLC. Recombinant hSCF samples treated in

different buffers were buffer-exchanged into buffer A (20 mM sodium acetate, pH 4.5). The samples were directly injected onto a TSK SP-5PW column (7.5 mm × 10 cm). The separation was accomplished by a linear gradient from 100% buffer A to 24% buffer B, which is buffer A containing 0.5 M sodium sulfate, at a flow rate of 1.0 mL/min for 30 min. The chromatography was monitored at both 230 and 280 nm. The HPLC system is an HP 1050Ti liquid chromatograph equipped with titanium pumps, and a multiple wavelength detector. The data were collected by ChemStation software with a PC-based computer system.

Peptide Mapping. SCF samples were digested by bovine TPCK-treated trypsin and by Asp-N endoproteinase (Boehringer Mannheim) in 20 mM Tris-HCl (pH 7.8) at an enzyme-to-substrate ratio of 1:50 for 18 h at 37 °C. The digest was injected immediately onto a narrowbore reverse phase C-4 (2.1 × 250 mm) column for Asp-N digests or onto a C18 (2.1 × 150 mm) column (Vydac; The Separation Group, Hesperia, CA) and separated using a gradient of 0.1% trifluoroacetic acid to 90% acetonitrile in 0.1% trifluoroacetic acid as described elsewhere (*10*). The flow rate was 0.25 mL/min with detector wavelengths set at both 215 and 280 nm. The HPLC system is an HP 1090 equipped with a Chemstation and a diode array detector.

Sequence Analysis and Mass Spectrometry. Amino acid sequence analysis of intact protein or peptides was performed on an ABI automatic sequencer (Models 477A or 470A) equipped with a Model 120A on-line PTH amino acid analyzer and a Model 900A data collection system (*7*).

On-line liquid chromatography−electrospray ionization mass spectrometry (LC−MS) of peptide samples was performed on a Sciex API-I00 mass spectrometer (Thornhill, Ontario, Canada). LC−MS analysis was performed by splitting the HPLC outlet line, with 20% going directly to the mass spectrometer. The scan range on the mass spectrometer was set from *m*/*z* 300 to *m*/*z* 1800, with an orifice voltage of 75 V, a step size of 0.15 Da, and a dwell of 0.5 ms. The chromatographic conditions for LC−MS were identical with those described in the peptide mapping analysis. Electrospray ionization quadrupole ion trap mass spectrometry (ESI-QIT-MS) was performed on a Finnigan MAT ion trap mass spectrometer (San Jose, CA) according to the procedures described (*54*). Samples collected in the RP-HPLC mobile phase were analyzed directly or concentrated to dryness in a polypropylene microcentrifuge tube and reconstituted in 15% acetonitrile in 0.1% TFA. Analysis was performed by flow injection at a flow rate of 0.1−0.2 μL/min. Mass spectra were collected in the positive ion mode scanning over mass ranges of 150−1500 Da. In MS−MS analyses of peptides, individual ions were selected in the ion-trap and fragmented with a relative collision energy of 27−29%. The naming system for fragment ions uses the traditional a, b, and c series of ions if the charge is retained on the N-terminus as well as x, y, and z series of ions if the charge is on the C-terminus, which are followed by a subscript number indicating the position of the fragmentation in the peptide backbone (*55*).

In Vitro Cell Proliferation Activity. Cell proliferation assays were performed by measuring [^{3}H]thymidine incorporation in human megakaryoblastic leukemia cell line UT-7 as described (*56*). The concentration of various SCF samples required to reach a half-maximal proliferative stimulation was obtained by plotting the incorporation of radioactivity by the cells versus the SCF concentration (ng/mL) added to the cell culture.

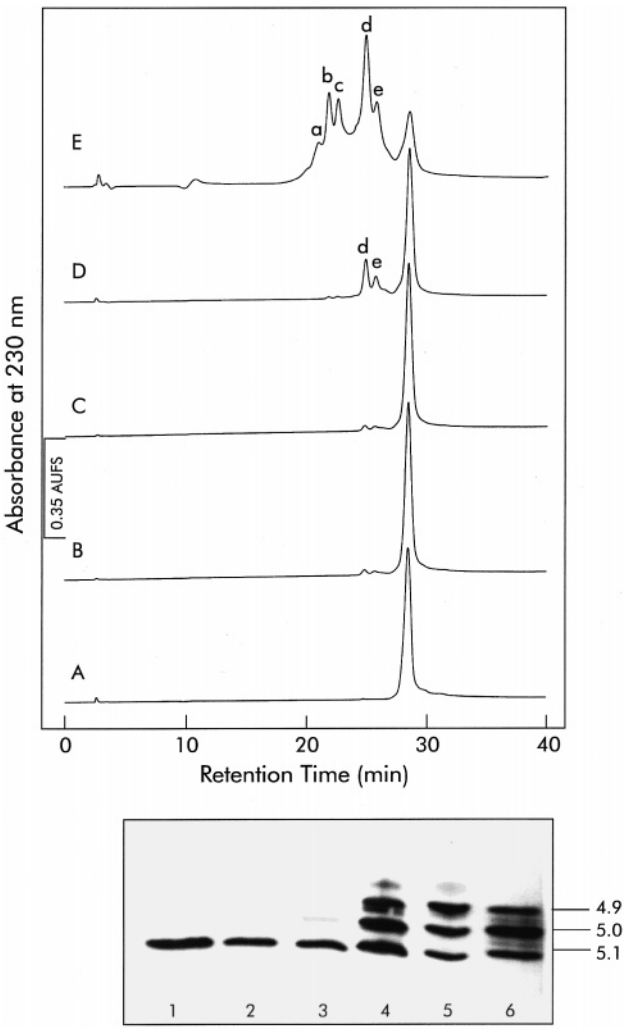

FIGURE 1: Top panel: Cation exchange HPLC of rhSCF samples. Recombinant hSCF in 1 mg/mL was incubated at 37 °C in 20 mM NaOAc, 140 mM NaCl, pH 5.0, for 1 day (A), in 10 mM sodium phosphate, pH 6.5, for 1 day (B), in 40 mM Tris-HCl, pH 7.2, for 1 day (C), in 100 mM $NaHCO_3$, pH 8.4, for 1 day ((D), and in 100 mM $NaHCO_3$, pH 8.4, for 5 days (E). An aliquot of each sample (25 μg) was injected for analysis. Bottom panel: IEF gel electrophoresis. Lane 1, standard rhSCF; lanes 2−4, samples in 20 mM sodium acetate, 140 mM NaCl, pH 5.0 (1 day); 10 mM sodium phosphate, pH 6.5 (1 day); and 100 mM $NaHCO_3$, pH 8.4 (5 days); lanes 5 and 6, isoforms d and e, respectively, isolated from cation exchange HPLC. Sample loading was 10−20 μg.

RESULTS

In Vitro Aging and Analysis of rhSCF Isoforms. Recombinant hSCF samples were incubated in various buffers at 37 °C to determine their stability during in vitro aging studies. Sulfopropyl cation-exchange HPLC was performed to analyze samples obtained from these incubation conditions at various time intervals. Figure 1 (top panel) illustrates chromatograms obtained from cation-exchange HPLC analysis of treated samples. After a 1 day incubation in 20 mM sodium acetate and 140 mM NaCl, pH 5.0, at 37 °C, the treated rhSCF exhibits chromatographic behavior not different from the original rhSCF sample (Figure 1, chromato-

gram A). Even after 5−7 days of incubation, the chromatographic profile remains unchanged, suggesting that rhSCF is stable at acidic buffers. Salt (NaCl) in the buffer does not show any effect on the stability. In both 10 mM sodium phosphate buffer, pH 6.5, and 40 mM Tris-HCl buffer, pH 7.2 at 37 °C, two early eluting SCF forms appear, each representing about 2% of the total material (Figure 1, chromatograms B and C). The levels of these forms increased to 5−7% after 5 days. However, in 100 mM sodium bicarbonate (pH 8.4) at 37 °C, these two early-eluting SCF species each represent approximately 5% of the total after 1 day incubation (Figure 1, chromatogram D). After 5 days of incubation under the same conditions, several early-eluting rhSCF forms, designated isoforms a, b, c, d, and e, became prominent, representing more than 60% of the total (Figure 1, chromatogram E). The half-life of rhSCF was estimated to be about 4.8 days in the sodium bicarbonate buffer, and is clearly much shorter than those observed at lower pH or other buffer conditions. Addition of NaCl in any of the conditions described above seems not to either enhance or reduce the formation of these acidic SCF forms.

The biological activity of rhSCF samples was evaluated by a cell proliferation assay. The in vitro activity for samples incubated in sodium acetate, sodium phosphate, or Tris-HCl for 5−7 days, as described above, is equivalent to that of rhSCF standard. Sample incubated in sodium bicarbonate buffer at alkaline pH has activity approximately 70−80% that of the original sample after 5 days. Note that under these conditions only about 40% of the original rhSCF remained, indicating that some of the early eluting forms still retained biological activity.

The early elution of isoforms in cation-exchange chromatography indicates that they are more acidic than the rhSCF standard. This is further demonstrated by IEF gel electrophoretic analysis as shown in Figure 1 (bottom panel). Freshly prepared rhSCF and sample incubated in 20 mM sodium acetate buffer containing 140 mM NaCl, pH 5.0 at 37 °C, for 1 day exhibit a single major IEF band with a p*I* estimated to be about 5.1 (lanes 1 and 2, respectively). Upon storage of rhSCF in 10 mM phosphate buffer (pH 6.5) at 37 °C for 1 day, a small amount of acidic species is present (lane 3). Large amounts of isoforms (two major and a minor acidic species) are generated when the sample was in sodium bicarbonate buffer for 5 days (lane 4). The two major acidic forms have p*I* values around 5.0 and 4.9. The minor form is more acidic than the major acidic forms, with a p*I* near 4.9.

Structural Characterization of rhSCF Isoforms. To further understand the structure of the isoforms, isolation and characterization of these acidic species were carried out. Approximately 1−2 mg of rhSCF sample was incubated in 100 mM $NaHCO_3$, pH 8.4, for 2 days, and the resulting rhSCF sample was subjected to SP-cation-exchange HPLC [see Figure 1 (top panel), chromatogram D]. Two major fractions, isoforms d and e, were analyzed for their IEF electrophoretic mobility as shown [Figure 1 (bottom panel), lanes 5 and 6]. These two fractions had indistinguishable IEF patterns; each contained three species corresponding to those of the original mixture (Figure 1, bottom panel, lane 4), except that the acidic isoform with a p*I* of 5.0 was the predominant species. One band at p*I* of 5.1 corresponds to that of the native protein, while the acidic bands represent

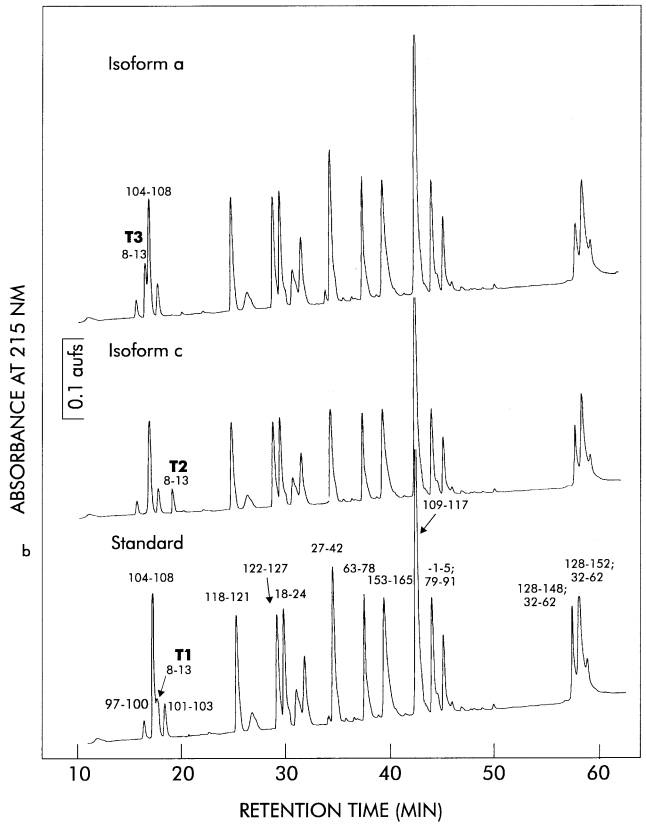

FIGURE 2: Tryptic peptide map analysis of rhSCF standard, isoform a, and isoform c. The numberings shown in the map of rhSCF standard represent the sequence positions assigned to the rhSCF sequence. Fifty micrograms of each digested sample was analyzed.

degraded rhSCF forms. Isoforms a, b, and c can also be isolated from samples incubated for 3−7 days [see Figure 1 (top panel), chromatogram E]. In IEF analysis, isoforms a and c exhibit major, discrete bands with p*I*'s of 4.9 and 5.0, respectively, while isoform b shows two bands at p*I* of 4.9 and 5.0, with equal intensity (data not shown).

Recombinant hSCF standard and the two early-eluting species, isoforms a and c, were digested with trypsin and the peptides characterized by electrospray LC−MS analysis. Figure 2 illustrates tryptic peptide maps for these forms. By on-line electrospray MS analysis plus sequence analysis of the isolated peptide fractions, most peptides as shown can be assigned to the rhSCF sequence including two disulfide bonds (i.e., Cys^4−Cys^{89} and Cys^{43}−Cys^{138}). In the map of the rhSCF standard, peptide T1 eluted as a shoulder peak as indicated and was confirmed to be a hexapeptide with a sequence of V-T-N-N-V-K (SCF sequence positions 8−13). In the map derived from isoform c, peptide T1 disappeared, and a new peptide T2 was detected. Peptide T2 had the sequence V-T-D-N-V-K. Apparently, peptide T2 shown in the map of isoform c must be derived from peptide T1 in the map of the rhSCF standard by conversion of Asn^{10} to Asp^{10}. The tryptic map obtained from isoform a indicated that the new peptide T3 eluted slightly earlier than peptide T1 which was missing in this map. N-Terminal sequence analysis confirmed that the peptide had a sequence of V-T-... and no sequence signals could be detected after the second sequencing cycle.

To further confirm their structural characteristics, peptides T1, T2, and T3 were subjected to ESI-QIT-MS analysis.

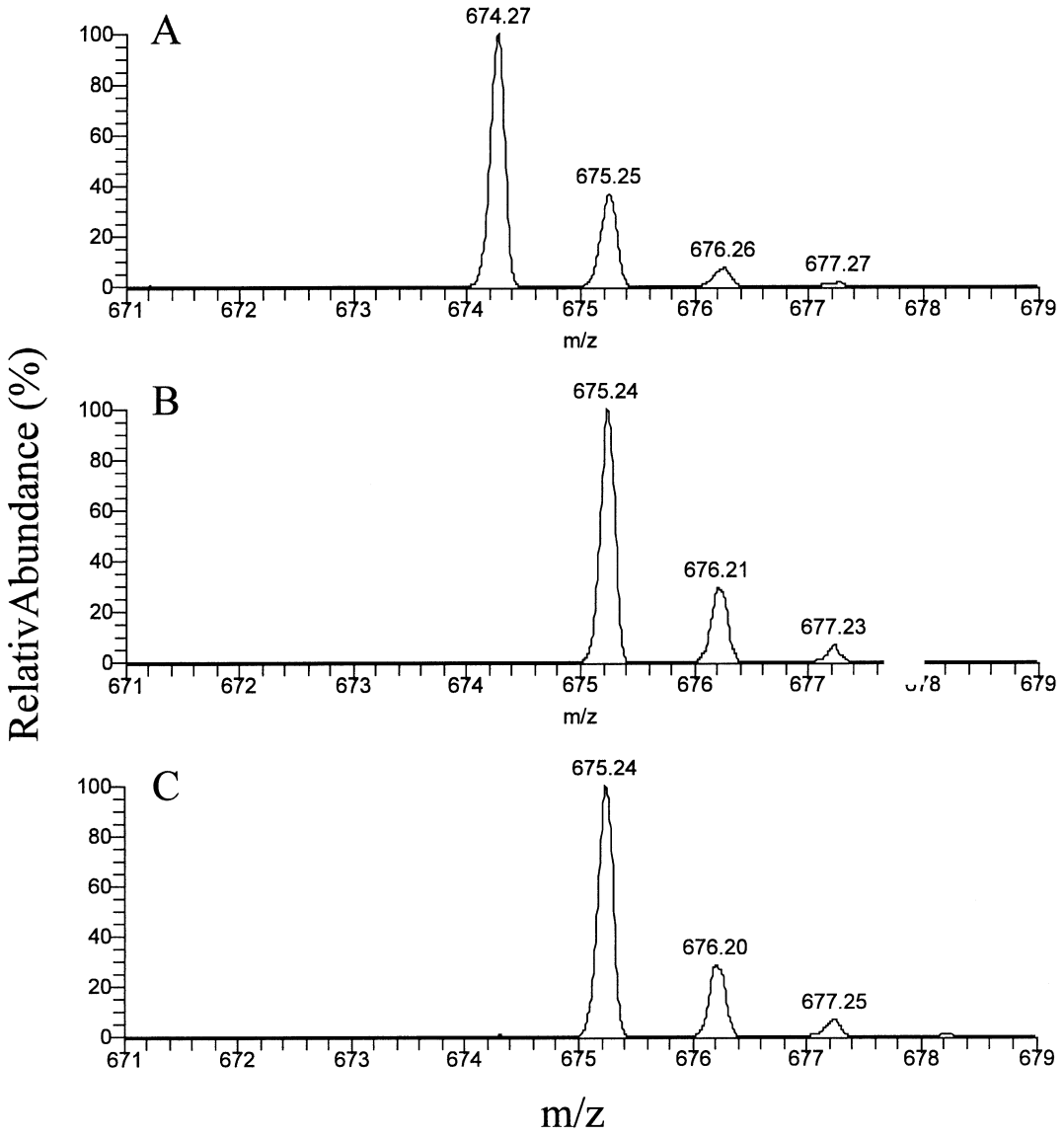

FIGURE 3: Molecular mass measurement of tryptic peptides T1, T2, and T3 by quadrupole electrospray ion-trap mass spectrometry. Note that the molecular ions are isotopically resolved.

Figure 3 shows spectra of the protonated monoisotopic molecular ions of these peptides obtained from zoom scan experiments. Isotopic resolution of the spectrum indicated that the molecular ion for peptide T1 is 674.27 Da and is singly charged. This observed ion mass is in close agreement with the theoretical mass of 674.4 Da calculated for the V-T-N-N-V-K sequence. Peptides T2 and T3 had identical masses of 675.24 Da which is 1 mass unit higher than peptide T1. The mass for peptide T2 is also in agreement with the theoretical mass of 675.3 Da obtained from the V-T-D-N-V-K sequence. From both mass determination and N-terminal sequence analysis, peptide T3 appears to have a sequence of V-T-X-N-V-K where X may represent a modified Asn residue. To account for the observed molecular ion and sequence determination, X must be an aspartic acid which forms a peptide bond linkage to the next Asn residue via a β-carboxyl side chain instead of the normal α-carboxyl group. An MS−MS analysis described below further confirmed this conclusion.

Each of the molecular ions shown in Figure 3 was subsequently subjected to MS−MS analysis as indicated in Figure 4. Amino acid sequences of both peptides T1 and T2 can be assessed with the assignment of several b and y series of ions. Due to the loss of ammonia from lysine or asparagine side chains, many of these ions generated ions with the loss of 17 Da as shown. In the mass spectrum of peptide T2, several b ions (b_4, b_5, and b_6), y ions (y_4, y_5, and y_6), and internal fragment ions (230.1, 313.3, and 329.2 Da) clearly exhibit one mass unit higher than those derived from peptide T1, indicating that an Asp residue in peptide T3 replaces an Asn residue in peptide T1 at the third sequence position. Shown in Figure 4C is the MS−MS spectrum of peptide T3. The fragment ions are almost identical with those of peptide T2 with the exception that signals of both y_3 (360.2 Da) and y_4 (475.2 Da) ions are significantly higher. The prominent y_3 and y_4 ions indicate that a higher fragmentation rate had occurred at the Thr−X and X−Asn bonds and this may explain why the 313.3 Da ion assigned as b ion for an internal fragment (sequence T-D-N with loss of water) in the spectrum of peptide T2 is significantly lower in intensity. The above MS−MS results clearly indicated that peptide T3 has a sequence similar to that of peptide T2. However, to explain that Edman sequencing of peptide T3 stopped at the second position, the third amino acid must be

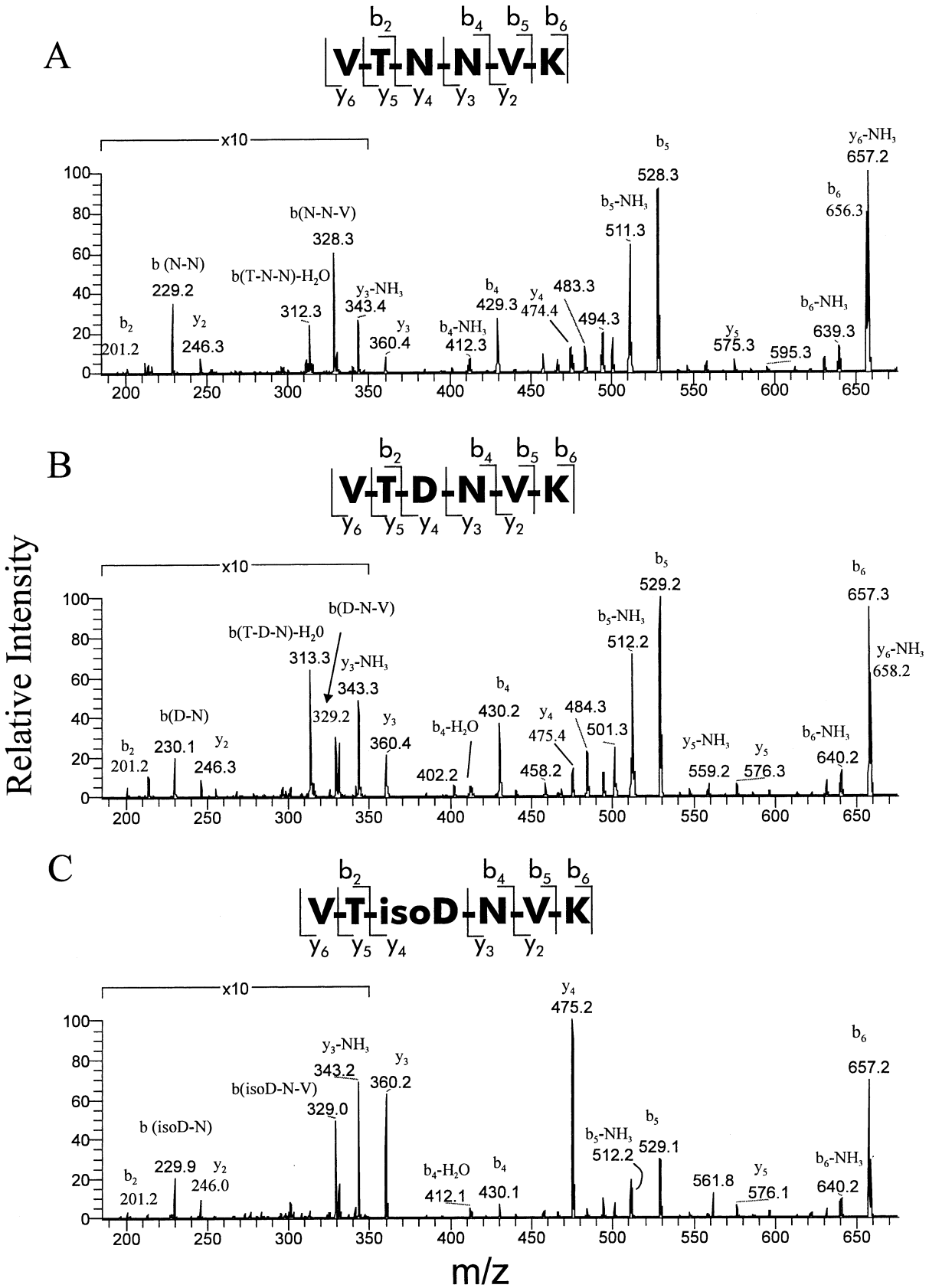

FIGURE 4: Sequence determination of tryptic peptides T1, T2, and T3 by MS−MS quadrupole electrospray ion-trap mass spectrometric analysis (panels A, B, and C, respectively). The assigned sequence and ion fragments are indicated. Ions at 229.2, 312.3, and 328.3 Da in panel A, at 230.1, 313.3, and 329.2 Da in panel B, and at 229.9 and 329.0 Da in panel C are the b series of ions for internal fragments as indicated.

an aspartic acid that links to the next Asn residue by a β-aspartyl peptide bond. Therefore, both sequence analysis and mass spectrometric data of the isolated peptides clearly confirmed that structures of isoform a, isoform b, and wild-type rhSCF were different at the 1 position, i.e., isoAsp, Asp, and Asn residues, respectively.

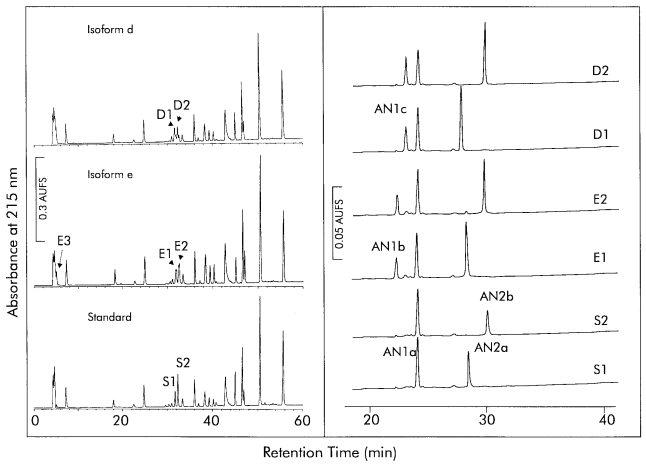

FIGURE 5: Left panel: Asp-N endoproteinase-derived peptide maps (50 μg) of rhSCF standard, isoform e, and isoform d. Right panel: Rechromatography of Asp-N endoproteinase-derived peptides S1, S2, D1, D2, E1, and E2 after DTT reduction.

In separate experiments, digestion of isoforms d and e with Asp-N endoproteinase was also performed. Figure 5 (left panel) illustrates a comparison of the Asp-N endoproteinase-derived peptide maps for the rhSCF standard and these two isoforms. Two peptide peaks at a retention time of about 32 min differed among these three maps. In the map of the rhSCF standard, two peptides, S1 and S2, elute as sharp peaks. Peak S1 contains an N-terminal peptide (residues [−1]−13) disulfide-linked to peptide 85−96 (Table 1). The structure of peptide S2 is identical with that of peptide S1 except that an additional Asp was found in peptide 84−96, suggesting that incomplete proteolytic cleavage of the Asp^{84}−Asp^{85} bond had occurred.

In the maps derived from isoforms d and e, two peptide fractions, designated D1 and D2 from isoform d as well as peptides E1 and E2 from isoform e, elute as doublet peaks. Peptides D1 and E1 were sequenced and shown to be the disulfide-containing peptides corresponding to peptide S1. Likewise, peptides D2 and E2 were equivalent to peptide S2 by sequence analysis. For further analysis, these peptides were reduced with DTT and subjected to reverse-phase HPLC (see Materials and Methods). Figure 5 (right panel) shows the chromatographic profiles. Peptide S1 generated two reduced peptides AN1a and AN2a, while peptide S2 generated AN1a and AN2b. As listed in Table 1, their sequences were determined to be as follows: AN1a, MEGICRNRVTNNK; AN2a, DLVECVKENSSK; and AN2b, DDLVECVKENSSK, using N-terminal sequence analysis and mass spectrometry. Reduction of peptide E1 generated peptides AN1a, AN1b, and AN2a, while reduction of peptide E2 generated AN1a, AN1b, and AN2b. The sequence of peptide AN1b was determined to be MEGICRNRVT, and its molecular mass is 1178.7 Da (calculated mass = 1178.6 Da), indicating that Thr is at the C-terminus. In addition to peptides E1 and E2, Asp-N digestion of isoform e also generated peptide E3, a tetrapeptide DNVK, that corresponds to residues 10−13 (Figure 5, left panel). The detection of peptides AN1b and E3 therefore indicates that there is an Asp-N proteolytic cleavage site due to the presence of an Asp residue at position 10. The coexistence of peptides AN1a and AN1b in the map of isoform e indicates the presence of two rhSCF sequences: a normal wild-type sequence and another sequence having Asn^{10} converted to Asp.

Reduction of peptides D1 and D2 isolated from isoform d consistently generated peptides AN1a, AN2a, and AN2b that are identical with those obtained from peptides S1 and S2. However, an additional peptide, AN1c, was also obtained from peptides D1 and D2. Edman sequencing showed that peptide AN1c contained a sequence, MEGICRNRVT, with no sequence signals detected after Thr. However, peptide AN1c had a protonated monoisotopic mass of 1634.7 Da, 1 mass unit greater than the value for the normal peptide AN1a (see Table 1). Since no sequence

Table 1: Structural Analysis of Disulfide Peptides after DTT Reduction and Reverse-Phase HPLC Peptide Mapping following Endoproteinase Asp-N Digestion of RhSCF Isoforms[a]

peptides	sequence determined by Edman degradation	mass[b] [MH^+]	sequence position	assigned sequence
S1[d]	MEGICRNRVTNNVK	2982.3 (2983.5)	[−1]−13	*f*
	DLVECVKENSSK		85−96	
S2[d]	MEGICRNRVTNNVK	3097.2 (3097.5)	[−1]−13	*f*
	DDLVECVKENSSK		84−96	
E3[e]	DNVK	−	10−13	*f*
AN1a	MEGICRNRVTNNVK	1633.5 (1633.8)	[−1]−13	*f*
AN1b	MEGICRNRVT[c]	1178.7 (1178.6)	[−1]−9	*f*
AN1c	MEGICRNRVT[c]	1634.7 (1634.8)	−[1]−13	MEGICRNRVT***isoD***NV
AN2a	DLVECVKENSSK	1350.6 (1350.7)	85−96	*f*
AN2b	DDLVECVKENSSK	1465.7 (1465.7)	84−96	*f*

[a] Except for peptides S1 and S2, all reduced peptides were obtained by rechromatography of the disulfide-containing peptides after DTT reduction shown in Figure 2 (right panel). [b] The protonated monoisotopic mass of the peptides was determined by electrospray mass spectrometry (see Materials and Methods). The numbers in parentheses are the theoretical values calculated based on the assigned sequences. [c] Sequence assignment of peptides AN1b and AN1c terminates at Thr by automatic Edman degradation. [d] Peptides S1 and S2 were isolated by peptide mapping of the rhSCF standard shown in Figure 5. [e] Peptide E3 was isolated by peptide mapping of isoform e (see Figure 5, left panel, chromatogram B). [f] The assigned sequence is identical with that obtained by N-terminal sequence analysis.

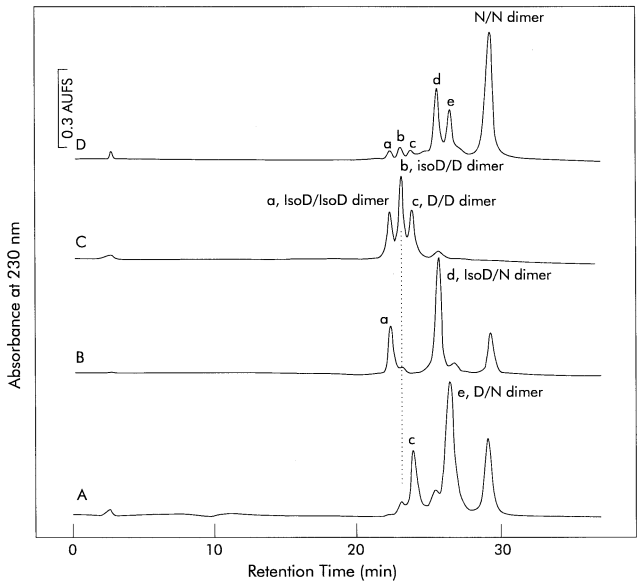

FIGURE 6: Cation exchange HPLC of isoform e (A), isoform d (B), isoform b (C), and rhSCF incubated in 100 mM $NaHCO_3$, pH 8.4, for 2 days at 37 °C (D). Aliquots of 20−50 μg were injected.

signal for peptide 2 was detected after Thr, we also conclude that the peptide is MEGICRNRVTXNVK, where X is the isoaspartyl residue, isoD. IsoD formation, derived from a transpeptidation reaction of Asp after deamidation of Asn^{10}, blocks Edman sequencing due to the presence of an atypical β-peptide bond. This modified peptide has a theoretical mass (MH^+) of 1634.8 Da which matches the experimental value (Table 1). Again, the coexistence of both peptides AN1a and AN1c in the map of isoform d indicates the presence of two rhSCF sequences: a normal wild-type sequence and another sequence having conversion of Asn^{10} to an isoaspartyl residue.

In solution, rhSCF exists as a noncovalently linked dimer. Isoforms a and c as described above are rhSCF homodimers since only a single SCF form was identified by peptide analysis. Isoform a is a homodimer containing an isoAsp residue at position 10, while isoform c is another homodimer containing an Asp at residue 10. Based on separate peptide analysis, each of the isoforms d and e (see Figure 5) generated two Asp-N peptides, i.e., peptides AN1a and AN1c from isoform d, and peptides AN1a and AN1b from isoform e. The sequencing yield for both peptides is similar. We conclude that rhSCF isoform d is a heterodimer containing an isoaspartyl monomer and a wild-type rhSCF monomer and isoform e is a heterodimer containing an aspartyl monomer and a wild-type rhSCF monomer. All of the Asn modifications occurred at position 10 in these forms. Isoform b, although not analyzed by peptide analysis, was confirmed to be another heterodimer containing both isoaspartyl and aspartyl monomers by dimer dissociation−reassociation studies of the isoform as described below. The detection of these rhSCF homodimers and heterodimers leads to the conclusion that deamidation of rhSCF at Asn^{10} occurred under in vitro aging conditions. The major deamidated products are rhSCF forms containing aspartic and isoaspartic acids.

Dimer Dissociation and Reassociation of rhSCF Isoforms. Our earlier studies have demonstrated that rhSCF dimer can rapidly undergo spontaneous monomer exchange (*14*, *15*).

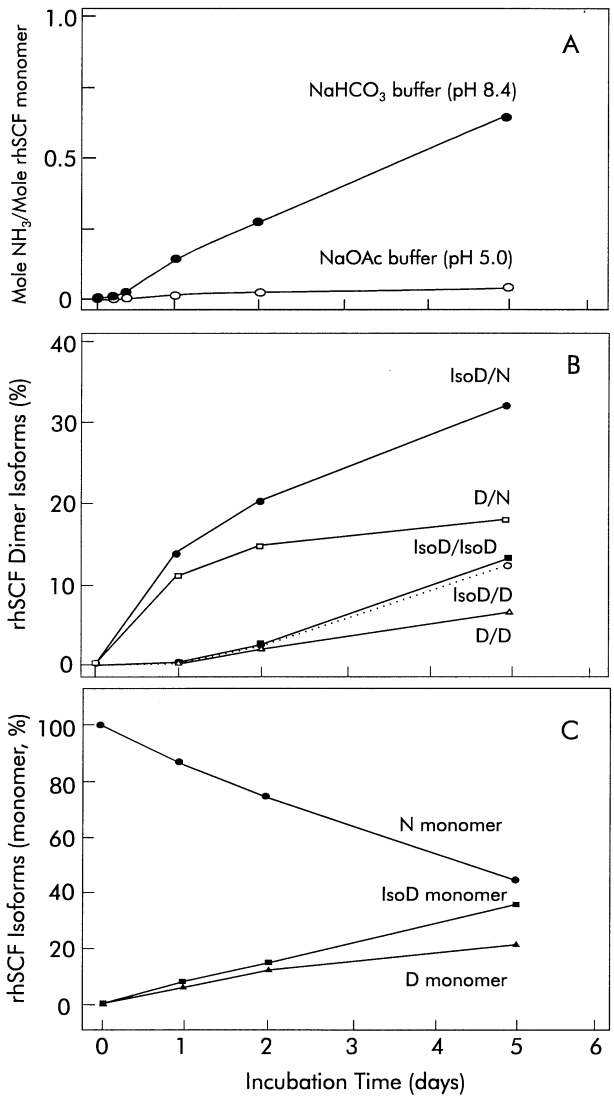

FIGURE 7: (A) Release of ammonia from rhSCF samples during deamidation experiments. (B and C) Rate of generation for rhSCF dimer isoforms and various forms of total monomers, respectively. Data were obtained from cation exchange HPLC of samples incubated in 100 mM $NaHCO_3$, pH 8.4 at 37 °C.

When rhSCF is mixed with an rhSCF variant, the formation of heterodimer can readily be detected by ion-exchange HPLC. This exchange phenomenon is also observed for the rhSCF-deamidated heterodimers, i.e., isoforms b, d, and e, as shown in Figure 6. For example, after isolation and a short period of incubation at room temperature (i.e., 4−6 h), D/N heterodimer (isoform e) can dissociate−reassociate to yield D/D (isoform c) dimer, D/N dimer, and N/N dimer at a ratio of approximately 1:2:1 (Figure 6A). The same redistribution occurs for isoform d (the isoD/N heterodimer) as shown in Figure 6B. In the case of isoform b, redistribution occurred into isoD/isoD dimer, isoform b, and D/D dimer with a ratio similar to that for isoforms d and e (Figure 6C). The data thus proved that isoform d is an IsoD/D heterodimer. The subunit redistribution was confirmed by the observed IEF profiles for isoforms d and e as seen in Figure 1 (lower panel, lanes 5 and 6). The samples had reached equilibrium subunit redistribution prior to the IEF. Thus, the band with p*I* 5.1 is N/N homodimer, the band with p*I* 4.9 is D/D homodimer (isoform d) or IsoD/isoD homodimer (isoform a), and the band at p*I* 5.0 is D/N

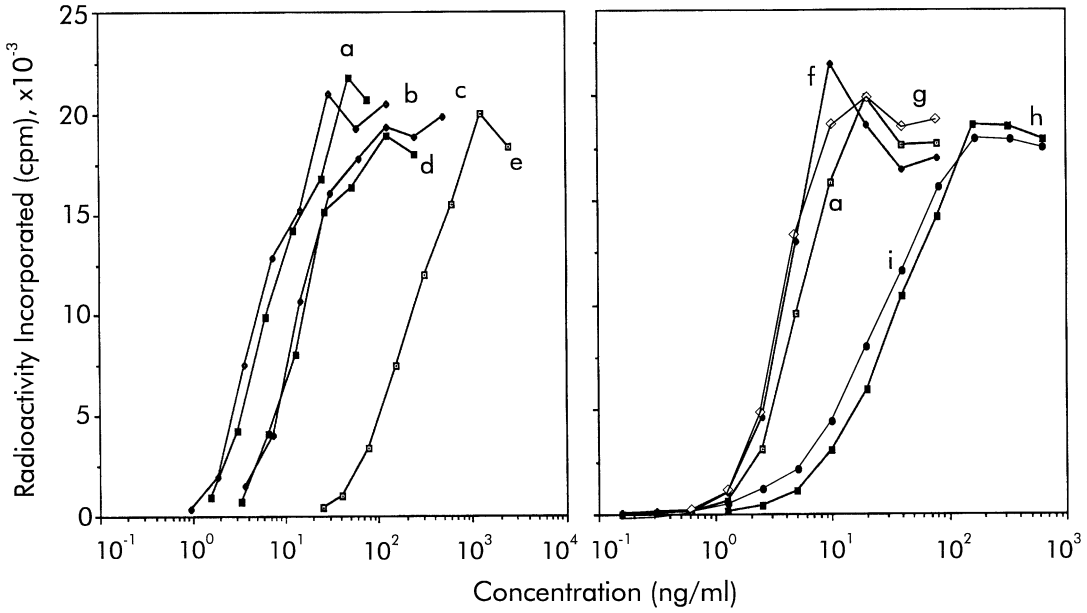

FIGURE 8: In vitro cell proliferation activity of rhSCF standard and various isoforms and variants. Stimulation of [^{3}H]thymidine uptake in cultured UT-7 cells was determined as a function of SCF concentration. Curve a, rhSCF standard; b, N/N dimer; c, isoD/D dimer; d, isoD/N dimer; e, isoD/isoD dimer; f, D/D dimer; g, N10 D variant; h, N10A variant; and i, N10E variant.

heterodimer (isoform e) or IsoD/N heterodimer (isoform d). Note that the distribution of species at any point during in vitro aging (e.g., Figure 1, top panel, chromatograms D and E, and Figure 6D) would reflect both deamidation and the ongoing subunit redistribution.

Deamidation Kinetics. In separate deamidation experiments, the amount of ammonia release was estimated by enzyme coupling assays (see Materials and Methods). As indicated in Figure 7A, no NH_3 was released in rhSCF samples incubated in 20 mM NaOAc buffer at pH 5.0. In contrast, approximately 0.65−0.70 mol of NH_3 per mole of rhSCF was released after 5 days of incubation in sodium bicarbonate at pH 8.4. The release of ammonia therefore reflects that more than 65% of the rhSCF sample has become deamidated.

Separation of rhSCF isoforms by ion-exchange chromatography (Figure 1) allows detailed kinetic analysis of isoform generation (Figure 7B, C). Figure 7B illustrates the rate of generation of isoforms in sodium bicarbonate buffer. IsoD/N species (isoform d) arises fastest and accumulates at the highest level, followed by D/N dimer (isoform e). Generation of isoD/isoD and isoD/D dimers (isoforms a and b) is slower but at a similar rate, while the D/D homodimer forms at the slowest rate. Figure 7C shows the disappearance rate for the nondeamidated monomers (N), as calculated from the sum of N/N homodimer, D/N heterodimer, and isoD/N heterodimer, and the generation rates for isoaspartyl and aspartyl subunits. After a 5 day incubation in sodium bicarbonate buffer, nondeamidated subunit remains at 42%, consistent with the release of ammonia indicated in Figure 7A. Generation of isoaspartyl subunit reaches about 37%, while aspartyl subunit reaches about 21%.

Biological Activity of rhSCF Isoforms and Variants. Cell proliferation of UT-7 megakaryocytic cells as measured by [^{3}H]thymidine uptake was performed to evaluate the in vitro biological potency for rhSCF and the isoforms. Figure 8 illustrates typical dose response curves for standard rhSCF (curve a) versus isolated N/N homodimer (curve b), isoD/D heterodimer (curve c), isoD/N heterodimer (curve d), isoD/isoD heterodimer (curve e), and D/D homodimer (curve f). IsoD/isoD homodimer is clearly the least active isoform, while the activities for isoD/D and isoD/N heterodimer are intermediate. SCF concentrations required to reach half-maximal stimulatory responses are compared in Table 2. Fully active rhSCF standard has a half-maximal stimulation concentration of 5.4 ng/mL. Comparatively, the isoD/isoD homodimer appears to have only 2% potency, while isoD/N and isoD/D heterodimers are about half as active as the standard rhSCF. The activity of D/D homodimer, however, is approximately 1.5-fold higher than that of the standard.

Table 2: Stimulatory Activity of RhSCF, Isolated Isoforms, and Variants in a Proliferation Assay Using UT-7 Megakaryotic Cells

proteins	half-max stimulation concn (ng/mL)[a]	activity (%)[b]
(A) isolated rhSCF-deamidated species		
standard	5.4	100
IsoD/isoD homodimer	280.0	2
IsoD/D heterodimer	13.0	42
IsoD/N heterodimer	13.8	39
D/D homodimer	3.7	148
D/N heterodimer	4.5	120
N/N homodimer	5.2	102
(B) rhSCF variants		
N10D variant	3.5	154
N10D/N11D variant	3.2	160
N10E variant	40.5	18
N10A variant	33.3	16

[a] See Figure 8 for the dose response curves. [b] Half-maximal stimulation concentration for standard rhSCF, divided by the value for isoform or variant, multiplied by 100.

Several rhSCF variants mutated at the Asn^{10} deamidation site were also prepared to evaluate their cell proliferation activity. Variant rhSCF forms, which include N10A, N10E, and N10D, have amino acid replacements for the labile Asn^{10}, while N10D/N11D variant contains an extra mutation at position 11. N10D variant is structurally identical to the rhSCF D/D homodimer isolated during aging studies; both

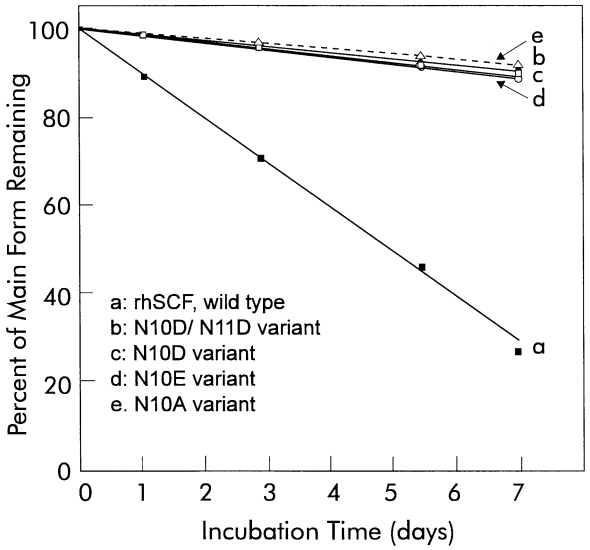

FIGURE 9: Comparative stability of rhSCF and variants. Samples were analyzed by cationic exchange HPLC for detection of deamidated and other forms. Samples were incubated in 100 mM sodium bicarbonate, pH 8.4, at 37 °C.

samples exhibited slightly higher stimulatory activity than rhSCF standard [Figure 8 (curves f and g) and Table 2]. The N10A and N10E variants showed 16% and 18% activity, respectively, relative to rhSCF standard [Figure 8 (curves h and i) and Table 2].

Stability of rhSCF Variants. Figure 9 illustrates stability studies of several rhSCF variants evaluated under in vitro aging conditions. During incubation in 100 mM sodium bicarbonate buffer (pH 8.4) at 37 °C, cation-exchange HPLC was used to quantify the amount of the remaining undegraded form. In comparison with the wild-type rhSCF, all four variants, i.e., N10A, N10E, N10D, and N10D/N11D, remain mostly undegraded as protein peaks were recovered equally well during incubation. These variant forms therefore exhibited good stability. In contrast to wild-type rhSCF, only very small fractions of isoaspartyl species (3−5%) were detected in the N10D and N10D/N11D variants after 5 days of incubation. Therefore, the rate of isomerization of Asp at position 10 in variant forms is significantly slower than during deamidation of Asn in the wild-type molecule.

DISCUSSION

In this report, we show that rhSCF undergoes rapid nonenzymatic deamidation in vitro under alkaline conditions. In addition to deamidation, there has been no indication for other modifications as a result of the in vitro aging process. A labile Asn residue (Asn^{10}) in the sequence, -TN^{10}NV-, was identified as the primary site for deamidation. Release of ammonia upon deamidation can be quantitatively measured as a function of time. Deamidation of Asn residue resulted in formation of an aspartic acid and generation of isoaspartate via isomerization of the aspartyl residue. Subunit exchange led to formation of rhSCF dimers with all possible combinations of isoaspartate, aspartate, and asparagine monomers during the in vitro aging process. In addition to the original unmodified N/N dimer, there are five homo- and heterodimeric species. These five species were detected as only two major acidic bands by narrow-range IEF gel electrophoresis (i.e., p*I* 4.9 for D/D, isoD/D, and isoD/isoD; p*I* 5.0 for D/N and isoD/N), indicating that aspartyl and isoaspartyl monomers are not resolvable by IEF analysis. The heterogeneity of these deamidated forms has been demonstrated by high-resolution ion-exchange HPLC analysis which separates deamidated samples into the five species discrete from the unmodified rhSCF. After isolation, deamidated heterodimers can further undergo dimer dissociation−reassociation, and three peaks including the original heterodimer can be obtained again after rechromatography. Kinetic data for generation of various deamidated monomers obtained from HPLC analysis are consistent with the rate of ammonia release determined enzymatically, suggesting that the HPLC method is applicable for quantification of rhSCF-deamidated forms.

In a number of cases, it has been shown that Asn-X sequences, particularly where X is Gly, Ser, or Ala, undergo β-aspartyl shift reactions in peptides and proteins, with rate constants corresponding to half-lives of 1 or 2 days, to yield isoAsp-X peptide products (*25*, *27*−*29*). As described (see the introduction), this modification reaction involves a succinimide intermediate that breaks down by two pathways to yield isomeric α- and β-aspartyl forms in a ratio of about 1:3. In rhSCF, the labile Asn residue in the -TN^{10}NV- sequence is flanked by Thr and Asn. The half-life for degradation of Asn^{10} is 4.8 days, suggesting that the -Asn−Asn- bond in SCF is slightly more stable than the -Asn−Gly (Ser, or Ala) bond in other proteins. Thr at the amino side of the deamidation site is one of the nearest neighbor residues showing a high frequency of inducing deamidation, while Asn at the carboxyl side does not appear to exhibit such an effect (*22*, *26*). The formation of both isomeric α- and β-aspartyl peptides is in a ratio of about 1:2, consistent with generation of a succinimide intermediate as described above. However, this intermediate was not detected in our analysis, probably because it is readily hydrolyzed under basic conditions (*25*). A similar degradation reaction also occurs in a 14-mer synthetic peptide having an rhSCF N-terminal sequence, suggesting that the -TNNV- sequence is prone to deamidation at the Asn residue penultimate to Thr at the N-terminus (our unpublished observation).

We observed that SCF variants with the replacement of Asn^{10} by Ala, Glu, or Asp generally exhibit much better stability. An acidic species derived from the N10D variant was detected only at a very low level (∼3%) after in vitro aging. Chromatographically, this acidic form coeluted with isoD/D heterodimer (data not shown), suggesting that the Asp^{10} residue in the variant form also undergoes isomerization reaction as observed in many other proteins (see the introduction). The isomerization rate, however, is very slow. N10E and N10A variants did not show such a structural change; however, the unmodified main HPLC peak was reduced to approximately 95% of its original level after 5 days of incubation, suggesting that other minor uncharacterized alterations had occurred as well.

It has been postulated that deamidation may play a role as a timer in protein turnover and in protein aging process (*35*, *40*). Formation of the β-aspartyl bond as a result of Asn deamidation or isomerization of Asp has been linked to changes in protein functions as described in the introduction. Similar effects were also found as a result of deamidation of rhSCF. Strikingly, for SCF the isoD/isoD homodimer retains only a small fraction of activity (2%),

indicating that formation of the β-aspartyl bond at the N-terminus of SCF leads to the loss of biological function. However, no changes in biophysical properties of this dimer can be detected by circular dichroism and fluorescence spectroscopy and by thermostability analysis, indicating no gross alteration of conformation (our unpublished data). In contrast to isoD/isoD dimer, the D/D homodimer exhibits activity higher than rhSCF standard. As shown in Figure 8C, the estimated distribution for isoaspartyl and aspartyl monomers predicted that the activity should be close to 76% of the rhSCF standard after 5 days of aging. This estimate is similar to the actual experimental value (see Results) and explains why the decrease in activity upon aging in alkaline buffer does not correlate with the rate of disappearance of the unmodified rhSCF form.

Confirming that the D/D homodimer is more active, N10D and N10D/N11D variants were found to be more active as well. The N10D/N11D variant matches canine SCF at these two sites, and canine SCF has higher activity than rhSCF in stimulating proliferation of UT-7 cells (our unpublished data). Variants with Ala or Glu replacing Asn^{10} had 5−10-fold reduced activity. These data suggest that the local conformation near the N-terminus of SCF may be critical for activity and that Asn or Asp at position 10 is optimal. Short truncations at the N-terminus of SCF have been demonstrated to adversely affect receptor binding and activity (*10*). Therefore, the observation of a critical region near the N-terminus of rhSCF has implications for the structure and function of rhSCF. SCF was predicted to have a typical cytokine fold with a four helical bundle structure (*57*). The N-terminal region (residues 1−11) is not involved in helix formation and is delimited by the Cys^4−Cys^{89} disulfide bond. A high propensity for β-turn formation is predicted for the sequence near the deamidation site. In addition to Asn^{10} and the N-terminal region, other functionally important regions of SCF near residues 79−95, Lys^{127}, and Asp^{128} have also been localized in studies with a neutralizing antibody (*16*, *58*). These regions may be structurally arranged to form a receptor binding surface for recognition of *KIT* receptor.

ACKNOWLEDGMENT

We are indebted to the Fermentation Process Development Group (Amgen, Thousand Oaks, CA) for performing bacterial fermentation and harvesting cell paste, to Mr. Ken Stoney and Mr. John Le for their technical help in the electrospray MS and LC-MS analyses, and to Ms. Joan Bennett for her help in typing the manuscript.

REFERENCES

1. Zsebo, K. M., Wypych, J., McNiece, I. K., Lu, H. S., Smith, K. A., Karkare, S. B., Sachdev, R. K., Yuschenkoff, V. N., Birkett, N. C., Williams, L. R., Satyagal, V. N., Bosselman, R. A., Mendiaz, E. A., and Langley, K. E. (1990) *Cell* 63: 195−201.
2. Martin, F. H., Suggs, S. V., Langley K. E., Lu, H. S., Ting, J., Okino, K. H., Morris, C. F., McNiece, I. K., Jacobsen, F. W., Mendiaz, E. A., Birkett, N. C., Smith, K. C., Johnson, M. J., Parker, V. P., Flores, J. C., Patel, A. C., Fisher, E. F., Erjavec, H. O., Herrera, C. J., Wypych, J., Sachdev, R. K., Pope, J. A., Leslie, I., Wen, D., Lin, C. W., Cupples, R. L., and Zsebo, K. M. (1990) *Cell* 63: 203-211.
3. Zsebo, K. M., Williams, D. A., Geissler, E. N., Broudy, V. C., Martin, F. H., Atkins, H. L., Hsu, R.-Y., Birkett, N. C., Okino, K. H., Murdock, D. C., Jacobsen, F. W., Langley, K. E., Smith, K. A., Takeishi, T., Cattanach, B. M., Galli, S. J., and Suggs, S. V. (1990) *Cell* 63: 213−224.
4. Williams, D. E., Eisenman, J., Baird, A., Rauch, C., Van Ness, K., March, C. J., Park, L. S., Martin, U., Mochizuki, D. Y., Boswell, H. S., Burgess, G. S., Cosman, D., and Lyman, S. D. (1990) *Cell* 63: 167−174.
5. Copeland, N. G., Gilbert, D. J., Cho, B. C., Donovan, P. J., Jenkins, N. A., Cosman, D., Anderson, D., Lyman, S. D., and Williams, D. E. (1990) *Cell* 63: 175−183.
6. Huang, E., Nocka, K., Beier, D. R., Chu, T.-Y., Buck, J., Lahm, H.-W., Wellner, D., Leder, P., and Besmer, P. (1990) *Cell* 63: 225−233.
7. Galli, S. J., Zsebo, K. M., and Geissler, E. N. (1994) *Adv. Immunol.* 55: 1−96.
8. Broudy, V. C. (1997) *Blood* 90: 1345−1364.
9. Lu, H. S., Clogston, C. L., Wypych, J., Fausset, P. R., Lauren, S., Mendiaz, E. A., Zsebo, K. M., and Langley, K. E. (1991) *J. Biol. Chem.* 266: 8102−8107.
10. Flanagan, J. G., Chan, D. C., and Leder, P. (1991) *Cell* 64: 1025−1035.
11. Arakawa, T., Yphantis, D. A., Lary, J. W., Narhi, L. O., Lu, H. S., Prestrelski, S. J., Clogston, C. L., Zsebo, K. M., Mendiaz, E. A., Wypych, J., and Langley, K. E. (1991) *J. Biol. Chem.* 266: 18942−18948.
12. Langley, K. E., Wypych, J., Mendiaz, E. A., Clogston, C. L., Parker, V. P., Farrar, D. H., Brothers, M. O., Satyagal, V. N., Leslie, I., Birkett, N. C., Smith, K. A., Baltera, R. F., Lyons, D. E., Hogan, J. M., Crandall, C., Boone, T. C., Pope, J. A., Karkare, S. B., Zsebo, K. M., Sachdev, R. K., and Lu, H. S. (1992) *Arch. Biochem. Biophys.* 295: 21−28.
13. Lu, H. S., Clogston, C. L., Parker, V. P., Wypych, J., Lee, T. D., Swiderek, K., Baltera, R. F., Jr., Patel, A. C., Brankow, D. W., Liu, X.-D., Ogden, S. G., Karkare, S. B., Hu, S. S., Zsebo, K. M., and Langley, K. E. (1992) *Arch. Biochem. Biophys.* 298: 150−158.
14. Hsu, Y.-R., Wu, G. M., Mendiaz, E. A., Syed, R., Wypych, J., Toso, R., Mann, M. B., Boone, T. C., Narhi, L. O., Lu, H. S., and Langley, K. E. (1997) *J. Biol. Chem.* 272: 6406−6415.
15. Lu, H. S., Chang, W.-C., Mendiaz, E. A., Mann, M. B., Langley, K. E., and Hsu, Y.-R. (1995) *Biochem. J.* 305: 563−568.
16. Mendiaz, E. A., Chang, D. G., Boone, T. C., Grant, J. R., Wypych, J., Aguero, B., Egrie, J. E., and Langley, K. E. (1996) *Eur. J. Biochem.* 239: 842−849.
17. Broxmeyer, H. E., Maze, R., Miyazawa, K., Carow, C., Hendrie, P. C., Cooper, S., Hangoc, G., Vadhan-Raj, S., and Lu, L. (1991) *Cancer Cells* 3: 480−487.
18. Morstyn, G. (1995) *Rev. Invest. Clin.* 47: 1−4.
19. Clark, S., Stephenson, R. C., and Lowenson, J. D. (1992) in *Stability of Protein Pharmaceuticals. Part A—Chemical and Physical Pathways of Protein Degradation* (Ahern, T. J., and Manning, M. C., Eds.) pp 1−29, Plenum Press, New York.
20. Liu, D. T. Y. (1992) *Trends Biotechnol.* 10: 364−369.
21. Wright, T. H. (1991) *Crit. Rev. Biochem. Mol. Biol.* 26: 1−52.
22. Clarke, S. (1987) *Int. J. Pept. Protein Res.* 30: 808−821.
23. Robinson, A. B., Scotcher, J. W., and MeKerrow, J. H. (1973) *J. Am. Chem. Soc.* 95: 8156−8159.
24. Geiger, T., and Clarke, S. (1987) *J. Biol. Chem.* 262: 785−794.
25. Stephenson, R. C., and Clarke, S. (1989) *J. Biol. Chem.* 264: 6164−6170.
26. Wright, H. T. (1991) *Protein Eng.* 4: 283−294.
27. Bornstein, P., and Balian, G. (1970) *J. Biol. Chem.* 245: 4854−4856.
28. Aswad, D. W. (1984) *J. Biol. Chem.* 259: 10714−10721.
29. Clarke, S. (1985) *Annu. Rev. Biochem.* 54: 479−506.
30. Johnson, A. B., Shirokawa, J. M., Hancock, W. S., Spellman, M. W., Basa, L. J., and Aswad, D. W. (1989) *J. Biol. Chem.* 264: 14262−14271.
31. Potter, S. M., Henzel, W. J., and Aswad, D. W. (1993) *Protein Sci.* 2: 1648−1663.

32. Di Donato, A., Ciardiello, M. A., Nigris, M. D., Piccoli, R., Mazzarella, L., and D'Alessio, G. (1993) *J. Biol. Chem.* 268: 4745−4751.
33. Sharma, S., Hammen, P. K., Anderson, J. W., Leung, A., Georges, F., Hengstenberg, W., Klevit, R. E., and Waygood, E. B. (1993) *J. Biol. Chem.* 268: 17695−17704.
34. Robinson, A. B., and Rudd, C. J. (1974) *Curr. Top. Cell. Regul.* 8: 247−294.
35. Gracy, R. W., Lu, H. S., Talent, J. M., and Yuan, P. M. (1983) in *Altered Proteins and Aging* (Adelman, R. C. and Roth, G. S., Eds.) Vol. 6, pp 9−34, CRC Press, New York.
36. Di Donato, A., and D'Alessio, G. (1981) *Biochemistry* 20: 7232−7237.
37. Voorter, E. C. M., Roersma, E. S., Blomendal, H., and de Jong, W. W. (1987) *FEBS Lett.* 221: 249−252.
38. Artigues, Birkett, A., and Schirch, V. (1990) *J. Biol. Chem.* 265: 4853−4858.
39. Manning, M. C., Patel, K., and Borchart, R. T. (1989) *Pharm. Res.* 6: 903−918.
40. Stadmann, E. R. (1990) *Biochemistry* 29: 6323−6331.
41. Yamada, H., Ueda, T., Kuroki, R., Fukumura, T., Yasukochi, T., Hirabayashi, T., Fujita, K., and Imoto, T. (1985) *Biochemistry* 24: 7953−7959.
42. George-Nascimento, C., Lowenson, J., Borissenko, M., Calderon, M., Medina-Selby, A., Kuo, J., Clarke, S., and Randolf, A. (1990) *Biochemistry* 29: 9586−9591.
43. Cacia, J., Keck, R., Presta, L. G., and Frenz, J. (1996) *Biochemistry* 35: 1897−1903.
44. Capasso, S., Di Donato, A., Esposito, L., Sica, F., Sorrentino, G., Vitagliano, L., Zagari, A., and Mazzarella, L. (1996) *J. Mol. Biol.* 257: 492−496.
45. Stevenson, C. L., Donlan, M. E., Friedman, A. R., and Borchardt, R. T. (1993) *Int. J. Pept. Protein Res.* 42: 24−32.
46. Chazin, W. J., Kordel, J., Thulin, E., Hofmann, T., Drakenberg, T., and Forsen, S. (1989) *Biochemistry* 28: 8646−8653.
47. Paranandi, M. V., Guzzetta, A. W., Hancock, W. S., and Aswad, D. W. (1994) *J. Biol. Chem.* 269: 243−253.
48. Tuong, A., Maftouh, M., Ponthus, C., Whitechurch, O., Roitsch, C., and Picard, C. (1992) *Biochemistry* 31: 8291−8299.
49. Tsai, P. K., Bruner, M. W., Irwin, J. I., Ip, C. C. Y., Oliver, C. N., Nelson, R. W., Volkin, D. B., and Middaugh, C. R. (1993) *Pharm. Res.* 10: 1580−1586.
50. Wingfield, P. T., Mattaliano, R. J., MacDonald, H. R., Craig, S., Clore, G. M., Gronenborn, A. M., and Schmeissner, U. (1987) *Protein Eng.* 1: 413−417.
51. Langley, K. E., Mendiaz, E. A., Liu, N., Narhi, L. O., Zeni, L., Parseghian, C., Clogston, C. L., Leslie, I., Pope, J. A., Lu, H. S., Zsebo, K. M., and Boone, T. C. (1994) *Arch. Biochem. Biophys.* 311: 55−61.
52. Clogston, C. L., Hsu, Y.-R., Boone, T. C., and Lu, H. S. (1992) *Anal. Biochem.* 202: 375−383.
53. Zale, S. E., and Klibanov, A. M. (1986) *Biochemistry* 25: 5432−5444.
54. Jonscher, K. R., and Yates, J. R. (1997) *Anal. Biochem.* 244: 1−15.
55. Biemann, K. (1990) *Methods Enzymol.* 193: 455−479.
56. Smith, K. A., and Zsebo, K. M. (1992) in *Current Protocols in Immunology* (Coligan, J. E., Kruisbeek, A. M., Margulies, D. H., Shevach, E. M., and Strober, W., Eds.) pp 6.17.1−6.17.11, John Wiley & Sons, New York.
57. Bazan, J. F. (1991) *Cell* 65: 9−10.
58. Matous, J. V., Langley, K. E., and Kaushansky, K. (1996) *Blood* 88: 437−444.

BI972372Z